

Quantum high-frequency conductivity oscillations in graphene multilayers and nodal semimetals in a tilted magnetic field

Juan Carlos Medina Pantoja¹, Juan Sotelo-Campos¹, and Igor V. Kozlov^{2,a}

¹ Universidad Peruana Cayetano Heredia, Departamento de Ciencias Exactas, Av. Honorio Delgado 430, 31 Lima, Perú

² B. Verkin Institute for Low Temperature Physics and Engineering of the National Academy of Sciences of Ukraine, 47 Nauky Ave., 61103 Kharkiv, Ukraine

Received 1 April 2017

Published online (Inserted Later) – © EDP Sciences, Società Italiana di Fisica, Springer-Verlag 2017

Abstract. A new type of angular oscillations of the high-frequency conductivity for conductors with a band-contact line has been predicted. The effect is caused by groups of charge carriers near the self-intersection points of the Fermi surface, where the electron energy spectrum is near-linear and can be described by anisotropic Dirac cone model. The amplitude of the resonance peaks satisfies the simple sum rule. The ease in changing the degree of anisotropy of the Dirac cone due to the angle of inclination of the magnetic field makes the considered type of oscillations attractive for experimental observation of relativistic effects.

1 Introduction

15 Recently, there has been growing interest in the study of
16 nodal semimetals having band-contact lines. First prin-
17 ciples calculations indicates the existence of ring-shaped
18 nodal lines in Ca, Sr, Yt [1]. Also, the topological tran-
19 sition $3\frac{1}{2}$ kind is known for the conductors with band-
20 contact line and thus possible in graphite conductors fam-
21 ily, Be, Mg, Zn, Cd, Al and other materials [2]. Usual
22 graphite have nodal lines [3].

23 In this paper we call attention to the effects of
24 anisotropic Dirac cones without an inversion center (tilted
25 Dirac cones) in nodal semimetals. The Hamiltonian, cor-
26 responding to the linear energy spectrum of Dirac-type
27 charge carriers has the form [4–6]:

$$\epsilon(p_x, p_y) = v_0(\alpha\sigma_x p_x + \sigma_y p_y + \eta p_y) \quad (1)$$

28 where the absence of an inversion center $\eta \neq 0$ is either a
29 consequence of the internal symmetry of the conductor or
30 may be achieved artificially, e.g. in strained graphene or
31 in a problem of Dirac electron drift in crossed electric and
32 magnetic fields [4]. The so-called “tilt” η can describe the
33 relativistic effects [7]. Furthermore, the “collapse” ($|\eta| >$
34 1) of the Hamiltonian (1) is naturally explained in terms
35 of relativistic rotations (“Lorentz boosts”) [8].

36 The implementation of the Hamiltonian (1) for
37 graphene requires a relatively strong electric fields
38 $\sim 10^6$ V/m and relatively large strain values in the sam-
39 ple $\sim 10\%$ [7]. In case of natural anisotropy, particularly in
40 the compound $\alpha-(BEDT-TTF)_2I_3$ [4,5,9–11], changing
41 of parameters of the electron energy spectrum is difficult,

42 since the latter is due to the intrinsic properties of the
43 conductor. Thus the experimental observation of effects
44 that require a parameter η to be changed is associated
45 with certain difficulties in these conductors. All the above
46 mentioned conductors have a pronounced two-dimensional
47 nature.

48 At the same time physical phenomena characteristic
49 of the Hamiltonian (1), will take place in nodal semimet-
50 als near the self-intersection points of Fermi surfaces. It
51 can be noticed that in a tilted magnetic field, the electron
52 energy spectrum in a Larmor orbit’s plane will be given
53 by the model (1), where the value of η which determines
54 the degree of anisotropy of the electron energy spectrum,
55 can be easily changed by simply changing the tilt angle
56 of a quantizing magnetic field. The attractiveness of the
57 graphite and its derivatives is determined by the fact that
58 for simple chemical compounds the high purity of the con-
59 ductor required for the observation of high harmonics of
60 the quantum cyclotron resonance [12] can be more easily
61 achieved.

62 The goal of the present work is new oscillation phe-
63 nomena caused by tilted Dirac cone effects in conductors
64 having band-contact (nodal) lines. In Section 2 we choose
65 the model of the electron energy spectrum. The model
66 has the qualitative accordance with the Fermi surface of a
67 number of nodal semimetals. The conditions limiting the
68 applicability of the model are given. In Section 3 a new
69 type of angular oscillations of the high-frequency conduc-
70 tivity for conductors with nodal lines has been predicted.
71 The physical mechanism of these oscillations is explained.
72 Section 4 shows that the amplitude of the resonance peaks
73 satisfies the simple sum rule or the “magic square rule”,
74 which follows directly from properties of Pauli matrices.

^a e-mail: kozlov@ilt.kharkov.ua

1 In Section 5 the paper is summarized and concluded. The
 2 possibility to observe the predicted oscillation effects is
 3 discussed. We provide a brief overview of articles related
 4 to the results of the present work.

5 2 Model

6 The model of graphene multilayers with a crystal lattice
 7 of AA type stacking is convenient for the observation of
 8 the resonant effects near the Dirac cone, since the charac-
 9 ter of the energy spectrum of the charge carriers can be
 10 considered to be linear in a broad range of energies [13,14].
 11 AA stacked graphite is unstable and cannot exist under
 12 natural conditions. Although the nanoparticles with the
 13 number of layers of about ten grown on the border of
 14 the diamond may be available for direct observation [15].
 15 Nevertheless, the energy spectrum of AA type graphite is
 16 widely used in theoretical works as the simplest and the
 17 most convenient theoretical model due to its characteris-
 18 tics, such as layering and Dirac energy spectrum of charge
 19 carriers near the Fermi surface (see the work) [13] (see also
 20 Ref. [16]). The Hamiltonian of low-energy charge carriers
 21 carriers corresponding to the model has the form:

$$H(\mathbf{p}) = v_{\parallel}(\sigma_x p_x + \sigma_y p_y) - 2t \cos\left(\frac{a_z p_z}{\hbar}\right), \quad (2)$$

22 where a_z is the interlayer distance and t is the overlap
 23 integral of the wave functions in adjacent layers, that we
 24 consider to be positive. This model was proposed for the
 25 conductors with a graphitelike energy spectrum (2) in refer-
 26 ence [13], where a linear magnetoresistance of a layered
 27 conductor with a small overlap integral t was investigated.

28 One can also easily see the qualitative accordance of
 29 the model (2) with a fragment of the Fermi surface of
 30 a number of nodal semimetals near the point of self-
 31 intersection of Fermi surfaces (see Fig. 1 of Ref. [2]). In
 32 particular the topological transition of $3\frac{1}{2}$ kind [2] occurs
 33 when $\epsilon_F = \pm 2t$ for the model (2).

34 This model of the electron energy spectrum can be
 35 also suitable for a number of graphite intercalates with
 36 AA type stacking of graphene layers [17]. For example,
 37 recent ARPES studies have reported about the direct ob-
 38 servation of a linear energy spectrum of charge carriers in
 39 KC_8 compounds. Along with the observed data concern-
 40 ing the traditional quantum oscillation effects, the ARPES
 41 results reveal the applicability of the Dirac cone model
 42 for the energy spectrum of the charge carriers in conduc-
 43 tors of this type [18]. The dependence of the energy of
 44 the charge carriers on the momentum components in the
 45 plane of the layers with a good degree of accuracy can
 46 be considered to be linear in the energy area of the order
 47 of fractions of eV, which is significantly higher than in
 48 graphite (several meV) [18,19]. The Fermi velocity in the
 49 layers plane $v_F \approx (0.82-0.97) \times 10^6$ m/s (see for exam-
 50 ple [12]), i.e. is close to the value of the Fermi velocity of
 51 conduction electrons in graphene. Unfortunately, a strong
 52 shift of the Fermi level is often observed in intercalated
 53 graphite. Therefore the Dirac singularity can be deep be-
 54 low the Fermi level, that takes place for intercalation by

55 alkali metals in particular. Nevertheless, the wide variety
 56 of intercalated graphite compounds gives the possibility
 57 to observe the effects of an anisotropic Dirac cone for the
 58 other members of this family of compounds. The model (2)
 59 was later used in reference [16] to study the quantum cy-
 60 clotron resonance in the case of not so high frequencies
 61 $\hbar\omega < \epsilon_1$, where ϵ_1 is the energy difference between the
 62 zeroth and first Landau levels, when the influence of the
 63 electron-hole transitions can be neglected.

64 In a tilted magnetic field $\mathbf{B} = (0, B_0 \sin \theta, B_0 \cos \theta)$,
 65 near the self-intersection point of the Fermi surface $\mathbf{p} =$
 66 $(0, 0, p_{z0})$, the dependence of the charge carriers energy on
 67 the components of the momentum in Larmor orbit's plane
 68 can be described by the expression (1) with the parameter
 69 values

$$\eta = -\frac{v_{\perp}}{v_{\parallel}} \tan \theta, \quad v_0 = v_{\parallel} \cos \theta, \\ \alpha = \frac{1}{\cos \theta}, \quad v_{\perp} = \frac{2ta_z}{\hbar} \sin \frac{a_z p_{z0}}{\hbar}, \quad (3)$$

70 (v_{\perp} is the Fermi velocity of conduction electrons along
 71 the normal to the layers). We assume that the inequal-
 72 ity $|\epsilon_F| < 2t$ holds, in which the Fermi surface has self-
 73 intersection points. We concentrate on the frequency re-
 74 gion $\hbar\omega > \epsilon_1$, so that the representation of the cyclotron
 75 resonance is determined by electron-hole transitions. The
 76 quantum cyclotron resonance and the classical contribu-
 77 tion to the high frequency conductivity in the frequency
 78 region $\hbar\omega \ll \epsilon_1$, where the influence of electron-hole tran-
 79 sition is negligible, have already been considered in refer-
 80 ence [16] for the case of the magnetic field normal to the
 81 layers. The deviation from the linear dependence (1) can
 82 be neglected for Landau levels with $\epsilon_n \sim \hbar\omega$, (A.1) for
 83 angles θ of the magnetic field \mathbf{B} satisfying the following
 84 inequality, which is considered to hold from now onwards:
 85

$$\epsilon_1 < \hbar\omega \ll \min\{\epsilon_1/\eta, (2t \pm \epsilon_F)\}. \quad (4)$$

86 We only consider the case of a sufficiently large relaxation
 87 time τ and relatively low temperatures T :

$$\frac{2t \pm \epsilon_F}{\hbar\omega} \ll \omega\tau \ll \frac{\hbar v_0}{a_z T \tan \theta}. \quad (5)$$

88 The right side of the inequality allows us to neglect the
 89 deviation from the linear dependence (1) in the region
 90 of temperature smearing of the Fermi surface (2), near
 91 the latter's points of self-intersection. Also later we will
 92 consider only the diagonal matrix elements of the con-
 93 ductivity tensor σ_{ii} in the plane (\tilde{x}, \tilde{y}) orthogonal to the
 94 vector \mathbf{B} ,

$$\tilde{x} = x, \quad \tilde{y} = y \cos \theta - z \sin \theta, \quad \tilde{z} = z \cos \theta + y \sin \theta. \quad (6)$$

95 Here in after the sign “tilde” will be used to denote
 96 the components in the rotated coordinate system (6).
 97 While calculating the conductivity tensor components, we
 98 will use quantum kinetic equation in the relaxation time
 99 approximation.

3 Conductivity tensor

Within the relaxation time approximation, the conductivity tensor $\sigma_{ij}(\omega)$ can be written in the form:

$$\sigma_{ij}(\omega) = \frac{2e^3 B}{(2\pi\hbar)^2 c} \sum_{n,m=-\infty}^{\infty} \int d\tilde{p}_z \left(-\frac{f_n^0(\tilde{p}_z) - f_m^0(\tilde{p}_z)}{E_n(\tilde{p}_z) - E_m(\tilde{p}_z)} \right) \times \frac{v_{mn}^j(\tilde{p}_z)v_{nm}^i(\tilde{p}_z)}{-i\omega + \frac{i}{\hbar}(E_n(\tilde{p}_z) - E_m(\tilde{p}_z)) + \frac{1}{\tau}}, \quad (7)$$

where $f_n^0(\tilde{p}_z) = f^0(E_n(\tilde{p}_z))$ is the Fermi-Dirac function, τ is the relaxation time, $v_{nm}^{i,j}$ are the matrix elements of the velocity operator and \tilde{p}_z is the projection of the momentum vector onto the magnetic field vector \mathbf{B} . The factor of 2 in the numerator is obtained from summation over the conventional spin. If the inequalities (4), (5) are satisfied, the energy levels for model (2) can be represented as

$$E_n(\tilde{p}_z) = \epsilon_1(\tilde{p}_z) \text{sign}(n) \sqrt{|n|} - 2t \cos \left(\frac{a_z \tilde{p}_z}{\hbar \cos \theta} \right) + \delta E_n(\tilde{p}_z). \quad (8)$$

Caused by the deviation from the model (1) the amendment $|\delta E_n(\tilde{p}_z)| \ll \frac{1}{\tau}$, does not significantly affect the position of the resonance peaks and can be omitted. The energy of the first Landau level

$$\epsilon_1(\tilde{p}_z) = v_{\parallel} \sqrt{2 \cos \theta \frac{eB\hbar}{c} \lambda^3(\tilde{p}_z)}, \quad (9)$$

where

$$\lambda(\tilde{p}_z) = \sqrt{1 - \left(\frac{2ta_z}{\hbar v_{\parallel}} \sin \left(\frac{a_z \tilde{p}_z}{\hbar \cos \theta} \right) \tan \theta \right)^2}, \quad (10)$$

can be easily obtained from the expression (A.1) with the energy spectrum parameters in (3) evaluated at the point $p_x = p_y = 0$, $p_z = \tilde{p}_z / \cos \theta$, and is given here for succession.

In the frequency region delimited by the inequalities (4) and (5), the conductivity oscillations will be determined by the charge carriers near the self-intersection points of the Fermi surface, for which the dependence of the cyclotron frequency $\hbar\Omega_n(\tilde{p}_z) = E_{n+1}(\tilde{p}_z) - E_n(\tilde{p}_z)$ on \tilde{p}_z can be neglected. Consequently, a real part of the conductivity tensor for this group of electrons can be written in the form:

$$\text{Re } \sigma_{ii}(\omega) \approx N \sum_{n,m} \frac{\sigma_{nm}^{ii}}{\frac{\tau^2}{\hbar^2} (E_n(\tilde{p}_{z0}) - E_m(\tilde{p}_{z0}) - \hbar\omega)^2 + 1}, \quad (11)$$

where N is the number of self-intersection points of the Fermi surface, $N = 2$ for the model (2). The magnitudes $E_{n,m}$ are evaluated by the expression (8) given at the self-intersection point of the Fermi surface $\tilde{p}_{z0} = p_{z0} \cos \theta$, $p_{z0} = \frac{\hbar}{a_z} \arccos \left(-\frac{\epsilon_F}{2t} \right)$. The approximate value of the conductivity tensor differs from the exact value, which takes into account all groups of electrons, by a correction

amendment $\Delta\sigma \ll \frac{t}{\hbar^2 \omega^2 \tau} \frac{e^2}{a_z}$, which is negligible in comparison with the characteristic values of the conductivity tensor (11) due to the left side of the inequality (5).

Each contribution σ_{nm}^{ii} is determined only by the transitions between the Landau levels with numbers n, m and correspond to the maximum of the conductivity $\text{Re } \sigma_{ii}(\omega)$ at the resonance frequency $\hbar\omega = \epsilon_n - \epsilon_m$ if the mutual overlap of the resonance peaks is omitted. In the region delimited by (4) only resonance frequencies corresponding to electron-hole transitions of the charge carriers are found where their energy spectrum are approximately linear. For the harmonics of the quantum cyclotron resonance with not too high order numbers

$$|n|, |m| \ll 1/(k^2 \eta^2), \quad k = |n| - |m|, \quad (12)$$

that means the linear approximation for the electron energy spectrum in the calculation of the matrix elements of the velocity operator, the contributions σ_{nm}^{ii} can be written in the form:

$$\sigma_{nm}^{ii} = \frac{2e^3 B \tau \cos \theta}{(2\pi\hbar)^2 c |v_{\perp}|} |v_{nm}^i|^2, \quad (13)$$

here v_{\perp} , (3) and v_{nm}^i (A.6) are determined by the linear energy spectrum (1) with the parameters (3) and (A.1) evaluated at $\mathbf{p} = (0, 0, p_{z0})$. The phase independence of the quantum oscillations of the conductivity tensor (11) and (13) on the Fermi energy under the conditions of quantum cyclotron resonance and the absence of temperature damping of the oscillations at not so high temperatures, when the electron-phonon scattering can be neglected, are associated with the fact that in case of the linear energy spectrum (1), the cyclotron frequency of the charge carriers of Dirac type depends strongly on the number of Landau levels, but is practically the same for charge carriers which have different momentum component along the magnetic field direction (see the part 4.C of the Ref. [20]). In case of a tilted magnetic field we can neglect the difference between the linear relation (1) and the exact energy spectrum within the limits of the temperature smearing of the Fermi level when inequality (5) is satisfied. In a quantized magnetic field orthogonal to the layers, the possibility of observing a high-temperature effect for the conductors of the graphite family was predicted in reference [16], where preliminary evaluations were provided.

Figure 1 shows the behavior of the diagonal components of the conductivity tensor as a function of the magnetic field magnitude for the fixed magnetic field tilt θ and frequency ω . The relation is numerically built taking into account all the groups of electrons, $-\frac{\pi\hbar}{a_z} < p_z \leq \frac{\pi\hbar}{a_z}$ using the expressions (2), (3), (7), (A.1) and (A.6). The similar dependence built using the approximate expression (11) with the same values of the parameters is not visually different from that one shown in the figure. The pair of numbers (n, m) at each peak in Figure 1 and its reflection $(-m, -n)$ correspond to the Landau level numbers and the most important contributions to σ_{nm}^{ii} (13) forming the shown resonant peak. In a tilted magnetic

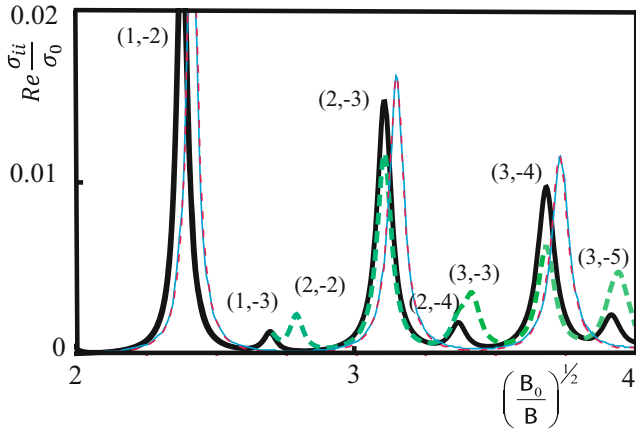


Fig. 1. The dependence of the conductivity tensor $\text{Re}\sigma_{xx}$ (continuous line) and $\text{Re}\sigma_{yy}$ (dashed line) on the magnetic field B for a constant electromagnetic field frequency, when $\tan\theta = 0$ (thin line) and $\tan\theta = 2/3$ (thick line). The constants used on the axes labels are $\sigma_0 = 2e^2/(\hbar a_z)$, $B_0 = \frac{c\hbar\omega^2}{2ev_{\parallel}^2}$. The parameter values used are $t/(\hbar\omega) = 8$, $\epsilon_F/(\hbar\omega) = 1$, $v_{\perp}/v_{\parallel} = 0.3$, $\omega\tau = 100$. The pairs of numbers (n, m) determine the numbers of a pair of Landau levels forming the given resonance peak.

1 field besides the main peaks $|n| - |m| = \pm 1$, which de-
 2 termine the representation of the cyclotron resonance for
 3 $\theta = 0$, higher harmonics are added. In these harmonics,
 4 the amplitude of the sufficiently high peaks of the pair
 5 (n, m) shows oscillations as a function of the angle θ . Figure
 6 2 shows the angular dependence of a resonance peak
 7 amplitude for a fixed frequency ω .

8 The physical mechanism of these oscillations can be
 9 explained as follows. The energy of the conduction elec-
 10 tron $\epsilon(\tilde{p}_x, \tilde{p}_y)$ in Larmor orbit's plane $\tilde{p}_z = \text{const.}$ can be
 11 described using the anisotropic Dirac cone model (1). It
 12 is well known, that the corresponding wavefunctions in a
 13 quantized magnetic field, which differ only by their Lan-
 14 dau level number n , can be expressed through the Hermi-
 15 tian functions (A.2) with shifted center X_n (A.4) which
 16 magnitude depends only on the Landau level number.
 17 Hence, when $|n|, |m| \gg 1$ the expressions for the com-
 18 ponent of the velocity operator $v_{n,m}^{\tilde{x},\tilde{y}}$ contain the prod-
 19 uct of oscillating functions having a phase shift caused
 20 by the difference $X_n - X_m \neq 0$, which depends on the
 21 magnitude and direction of the magnetic field \mathbf{B} . Their
 22 interference leads to the oscillatory dependence $v_{n,m}^{\tilde{x},\tilde{y}}$ (15),
 23 and, therefore, to the oscillations of the conductivity ten-
 24 sor component.

25 The representation of the oscillations of the conduc-
 26 tivity tensor (13) would be clearer if we use asymptotic
 27 expressions for the velocity operator. One can admit that
 28 for the velocity operator components $v_{n,m}^{\tilde{x},\tilde{y}}$ [6], which are
 29 related to the electron-hole transitions $\text{sign}(n) \neq \text{sign}(m)$
 30 and limited by the condition

$$|n| - |m| \ll 1/\eta, \sqrt{|n|}, \quad (14)$$

31 the known asymptotic expression $L_j^\alpha(x) \approx J_\alpha(2\sqrt{jx})$ can
 32 be applied yielding the components' simple asymptotic

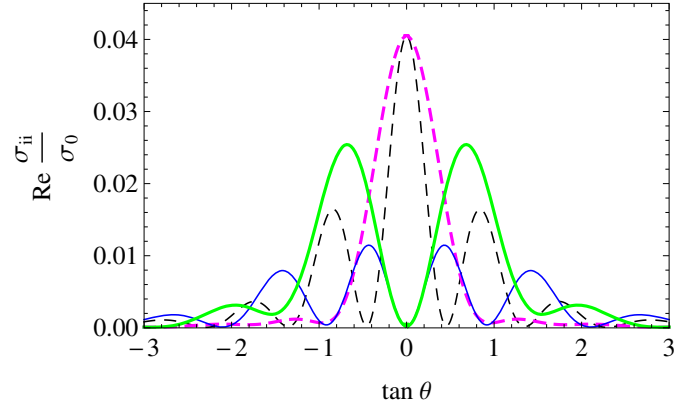


Fig. 2. The angular dependence of the maximum value of $\text{Re}\sigma_{yy}$ (thick line) and $\text{Re}\sigma_{xx}$ (thin line) near the resonance $(3, -4)$ (dashed line) and $(2, -4)$ (continuous line), normalized by the constant $\sigma_0 = 2e^2/(\hbar a_z)$, for a fixed value of the electromagnetic wave frequency ω . The parameter values used are $t/(\hbar\omega) = 7$, $\epsilon_F/(\hbar\omega) = 1.8$, $v_{\perp}/v_{\parallel} = 0.3$, $\omega\tau = 300$.

expression:

$$v_{nm}^{\tilde{y}} \approx v_0\lambda^2 J'_{|k|}(4\eta l), \quad v_{nm}^{\tilde{x}} \approx iv_0\lambda\alpha \frac{k}{4\eta l} J_{|k|}(4\eta l), \quad (15)$$

where $k = |m| - |n|$, $l = \min(|m|, |n|)$ and $J'_k(x)$ is the
 34 derivative of the Bessel function. The asymptotic form of
 35 the velocity operator components is insignificantly differ-
 36 ent from (A.6) for the physical picture of the oscillations
 37 phase shift and does not account for the overwhelming
 38 multiplier $\exp(-2\eta^2 l) \approx 1$ when $\eta \ll \frac{1}{\sqrt{|n|}}$, as the con-
 39 dition (4) holds true. A more accurate, though awkward,

40 the asymptotic expansion for associated Laguerre poly-
 41 nomials $L_n^\alpha(z)$, in particular, for the oscillatory behavior
 42 of the region $0 < z < 4n + 2(a + 1)$, can be found in
 43 reference [21]. The expressions (15) maintain the physical
 44 structure of the velocity operator oscillations. This is the
 45 way the asymptotic value of $v_{nm}^{\tilde{x},\tilde{y}}$ (15), as well as its exact
 46 expression (A.6), will be significantly different from zero
 47 only in the region of $|\eta| < \frac{|k|}{|n|+|m|}$, and exponentially lit-
 48 tle beyond it (this condition is easier to obtain using the
 49 WKB approximation in conjunction with the method of a
 50 stationary phase). Figure 3 shows the dependence of the
 51 resonance peaks amplitude (13) on m and n numbers. The
 52 oscillations of values σ_{ii}^{nm} are the result of the anisotropy
 53 of the energy spectrum of Dirac type that is indirectly
 54 confirmed by qualitative similarity of the given figure and
 55 Figures 2a and 2c of reference [4]. While constructing Fig-
 56 ure 3 the exact expressions for the matrix elements of the
 57 velocity operator v_{nm}^i for the energy spectrum (1) were
 58 used, however replacing them with the approximate val-
 59 ues (15) describes correctly the oscillation dependence of
 60 the peak amplitude in terms of inequality (14).
 61

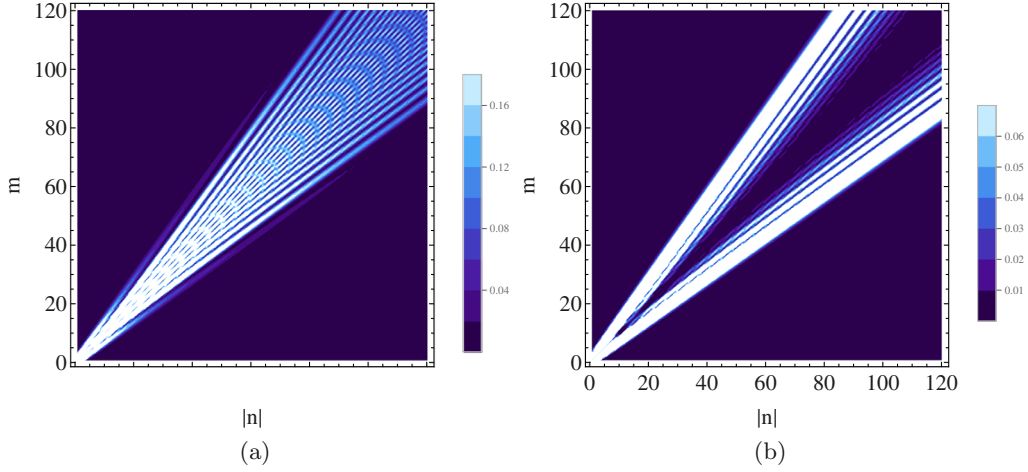


Fig. 3. The dependence of the contributions $\sigma_{nm}^{\tilde{y}\tilde{y}}$ (a) and σ_{nm}^{xx} (b), normalized by σ_{Σ} (17), that determine the conductivity tensor components (11) under the resonance conditions $\hbar\omega = \epsilon_n - \epsilon_m$ at the fixed magnitude and direction of the magnetic field, $\tan \theta = 0.3$, $v_{\perp}/v_{\parallel} = 0.3$, on the numbers (n, m) , which determine the resonances caused by electron-hole transitions.

4 Sum rule

The tilt angle of the magnetic field θ , corresponding to the condition $\eta(\theta) \sim 1/l$, separates the two cases of the quantum cyclotron resonance. At the smaller angles θ , the quantum cyclotron resonance will be determined only by the fundamental harmonics of $k = |n| - |m| = \pm 1$. For the larger angles θ , in the frequency range (4) a lot of higher resonance harmonics will appear, while the amplitude of the fundamental harmonics caused by electron-hole transitions $n + m = \pm 1$ falls sharply.

It may be noticed, that there is a kind of rule of conservation of the resonance peaks of total amplitude, explaining the decrease of the amplitude of the fundamental resonances during the appearance of higher harmonics. Namely, for an arbitrary η and $n = \text{const}$ the relation:

$$\sum_{m=-\infty}^{\infty} |v_{nm}^{\tilde{x}}|^2 = v_0^2 \alpha^2, \quad \sum_{m=-\infty}^{\infty} |v_{nm}^{\tilde{y}}|^2 = v_0^2 (1 + \eta^2), \quad (16)$$

is valid, which follows directly from the properties of the Pauli matrices $\sigma_{x,y}^2 = 1$. The expressions (16) remain valid when using the asymptotics (15) and pass to the known sum rule $J_0^2(x) + 2 \sum_{n=1}^{\infty} J_n^2(x) = 1$. From the expressions (13) and (16) it follows that the maximums of the cyclotron resonance peaks due to the charge carriers near the Dirac singularity (4), (12) obtained for the same values of magnitude and direction of the magnetic field \mathbf{B} (with different resonance frequencies ω) satisfy the relationship

$$\begin{aligned} \sum_{m=-\infty}^{\infty} \sigma_{nm}^{\tilde{x}\tilde{x}} &= \alpha^2 \sigma_{\Sigma}, \\ \sum_{m=-\infty}^{\infty} \sigma_{nm}^{\tilde{y}\tilde{y}} &= (1 + \eta^2) \sigma_{\Sigma}, \\ \sigma_{\Sigma} &= \frac{2e^3 B \tau v_0^2 \cos \theta}{(2\pi\hbar)^2 c |v_{\perp}|}, \end{aligned} \quad (17)$$

in which summed contributions visually correspond to one of the horizontal in Figure 3. So we have the following “magic square rule” for a table built from the resonance peak amplitude values of the conductivity σ_{nm} (17): the sums of all the elements in the rows ($n = \text{const.}$) and columns ($m = \text{const.}$) do not depend on their numbers and they are equal.

5 Conclusions

The found oscillatory dependence of the conductivity tensor (11), (13), (15) has a quantum interference nature and is a consequence of the anisotropy of the electron energy spectrum in Larmor orbit’s plane, which arises in a tilted magnetic field. The amplitude of the resonance peaks satisfies the simple sum rule or the “magic square rule”, which follows directly from properties of Pauli matrices. The character of the oscillatory dependence is similar to those observed in reference [4] oscillations of the absorption coefficient of the electromagnetic field for a two-dimensional conductor of Dirac type with a natural anisotropy of the electron energy spectrum, or in crossed electric and magnetic fields, as a function of an electric field or the degree of deformation of the conductor. Unlike the two-dimensional case, in graphite family conductors the degree of the Dirac cone anisotropy η can be modified by simply changing the inclination angle of a quantized magnetic field, which substantially facilitates the conditions for the experimental observation of oscillatory phenomena that are related to the Dirac cone anisotropy.

Providing that the charge carrier velocity in the plane of the layers v_0 (2) is close to its value in graphene (see, for example, Tab. 2 in Ref. [22]), the resonance frequency corresponding to the transition between zeroth and the first Landau levels $\omega \sim 5 \times 10^{13} \times \sqrt{B[\text{T}]} [\text{Hz}]$, when the magnetic field is directed by the normal to the layers, and decreases if magnetic field tilt angle θ is increasing according

1 to the expression (A.1). Thus, the region of the resonance
 2 frequencies in Figure 1 will be limited to the submillimeter
 3 and infrared diapason. Although the model (2) is suitable
 4 for multilayers of graphene with a AA type of stacking
 5 of the crystal lattice, but it can also be used for the de-
 6 scription of the physical properties of other anisotropic
 7 conductors with a Dirac singularity in the electron energy
 8 spectrum, the characteristics of which may differ much
 9 from the similar values in graphene, including the region
 10 of resonance frequencies. However, the observed oscilla-
 11 tory effect is not restricted by the given model and can
 12 take place in different conductors with nodal line in the
 13 energy spectrum. In particular, the energy spectrum of
 14 graphite with AB type of stacking is also characterized by
 15 a non-zero Berry phase [3] and has a local structure (1)
 16 in the proximity of self-intersection points of the Fermi
 17 surface [23,24]. The purity of highly oriented pyrolytic
 18 graphite (HOPG) gives the possibility of experimental ob-
 19 servation of higher harmonics of the quantum cyclotron
 20 resonance [12] and the angular oscillations of the kinetic
 21 coefficients in the frequency domain of the electromagnetic
 22 wave of millimeter and infrared range (see, for example
 23 Ref. [25] and references therein). The investigation of the
 24 angular oscillations of high-frequency kinetic coefficients
 25 which are caused by the charge carriers of Dirac type in
 26 graphite of AB type stacking is beyond the scope of this
 27 article and will be presented in a separate paper.

28 The absence of an inversion center ($\eta \neq 0$) of the
 29 model (1) in Larmor orbit's plane, being the cause of
 30 the oscillatory dependence on the matrix elements of the
 31 velocity operator (15), though does not lead to quanti-
 32 tative changes of the quantized energy spectrum (A.1).
 33 Therefore, the interference mechanism observed here may
 34 take place in the kinetic coefficients, which are related
 35 to electron transport phenomena (electrical conductiv-
 36 ity, impedance) and at the same time can not cause the
 37 magneto-angular oscillations of the density of states and
 38 the related thermodynamic characteristics of a conductor.
 39 Naturally the effects specific to a Dirac anisotropic spec-
 40 trum are not limited to high-frequency transport phenom-
 41 ena. Thus the phase transition of $3\frac{1}{2}$ kind in conductors
 42 with nodal lines in the energy spectrum of charge carriers,
 43 which is sensitive to the anisotropy of the Dirac electron
 44 energy spectrum, is described in reference [2].

45 The magneto-angular oscillations in bilayer graphene
 46 predicted in reference [26] have a similar physical nature
 47 as they are explained by interference of wave functions
 48 with the displacement of the centers of Larmor orbits in
 49 the graphene neighboring layers. However, the effect leads
 50 to the occurrence of the magneto-angular oscillations in
 51 the density of states of the electronic subsystem, which
 52 differs it from the mechanism of oscillations appearance
 53 Figure 2. Also in contrast to oscillations of the conductiv-
 54 ity tensor (11), (13), (15), which period of oscillations is
 55 determined by the ratio of the Fermi velocities in direc-
 56 tions perpendicular and parallel to the layers, the overlap
 57 integral between the layers does not affect the phase of
 58 the oscillations [26], although determines their amplitude.
 59 While working over the present article, we came across

reference [27], where type-II Weyl semimetals in a tilted
 magnetic field were investigated and Landau quantization
 was proved to be possible even in the given conductors
 for magnetic field directions with the effective tilt $\eta < 1$.
 The existence of a new type of angular oscillations of ki-
 netic coefficients for the conductors of the graphite family
 considered in the presented work was announced in the
 abstract [28].

The authors express the gratitude to FINCYT and CON-
 CYTEC of Peru for financial support of this work.

Author contribution statement

The contributions of the three authors are equal.

Appendix A: Matrix elements of the velocity operator

The eigenvalues ϵ_n and wave functions $\varphi_\nu(\mathbf{r})$ of the
 Hamiltonian (1) in a quantized magnetic field with the
 gauge $A = (0, By, 0)$ have the form:

$$\epsilon_n = v_0 \text{sign}(n) \sqrt{2 \frac{eB\hbar}{c} \lambda^3 \alpha |n|}, \quad (\text{A.1})$$

$$\begin{aligned} \varphi_\nu(x, y) = & \frac{(\alpha\lambda)^{1/4}}{2(2\pi\hbar)\sqrt{a_H}} \sqrt{\frac{1+\delta_{0,n}}{1+\lambda}} \\ & \times \exp\left(\frac{i}{\hbar} P_y y\right) \left\{ \left[\begin{array}{c} i\eta \\ 1+\lambda \end{array} \right] h_{|n|} \left(\frac{\sqrt{\alpha\lambda}}{a_H} (x+X_n) \right) \right. \\ & \left. - \left[\begin{array}{c} i(1+\lambda) \\ \eta \end{array} \right] \text{sign}(n) h_{|n|-1} \left(\frac{\sqrt{\alpha\lambda}}{a_H} (x+X_n) \right) \right\}, \end{aligned} \quad (\text{A.2})$$

where $\nu = (n, P_y)$ is the complete quantum index set, \mathbf{P}
 is the canonical momentum, the magnetic length

$$a_H = \sqrt{\frac{\hbar c}{eB}}, \quad \lambda = \sqrt{1-\eta^2}, \quad (\text{A.3})$$

the negative values of the Landau level numbers corre-
 spond to holes in the energy spectrum of charge carriers,

$$X_n = a_H \eta \text{sign}(n) \sqrt{\frac{2|n|}{\alpha\lambda}} - \frac{cP_y}{eB} \quad (\text{A.4})$$

is the centre of Larmor orbit of the conduction electrons,

$$h_n(\xi) = \frac{1}{\sqrt{2^n \sqrt{\pi} n!}} \exp(-\xi^2/2) H_n(\xi) \quad (\text{A.5})$$

is the solution of the dimensionless harmonic oscillator
 problem, $H_n(\xi)$ is the n th Hermite polynomial and $\delta_{0,n}$
 is the Kronecker symbol. It is considered that the con-
 tribution containing $\text{sign}(n)$, (A.2) is equal to zero when
 $n = 0$.

1 The matrix elements of the velocity operator compo-
2 nents have the form

$$v_{nm}^y = \lambda(\Phi_{nm} + \Phi_{mn}), \quad v_{nm}^x = i\alpha(\Phi_{nm} - \Phi_{mn}) \quad (\text{A.6})$$

3 where

$$\begin{aligned} \Phi_{nm} = & v_0 \lambda \sqrt{\frac{|n|}{2^{|m|-|n|+1}}} \sqrt{\frac{|m|!}{|n|!}} \Delta_{nm}^{|n|-|m|-1} e^{-\Delta_{nm}^2} \\ & \times L_{|m|}^{|n|-|m|-1}(2\Delta_{nm}^2) \text{sign}(n) \end{aligned} \quad (\text{A.7})$$

$$\Delta_{nm} = \frac{\eta}{\sqrt{2}} \left(\text{sign}(n) \sqrt{|n|} - \text{sign}(m) \sqrt{|m|} \right), \quad (\text{A.8})$$

4 when $n \neq 0$ and $\Phi_{0m} = 0$.

5 The expressions similar to (A.1), (A.2), (A.6) are given
6 in a series of works (for example, see [4,5]). In particular,
7 the expression (A.6) corresponds to the formulae (A1)–
8 (A2) of references [6] where the value of the parameter
9 $\alpha = 1$, if the dependence on the latter is considered by
10 simple coordinate transformation $y' = y$, $x' = x/\alpha$.

11 References

- 12 1. Motoaki Hirayama, Ryo Okugawa, Takashi Miyake,
13 Shuichi Murakami, Nat. Commun. **8**, 14022 (2017)
- 14 2. G.P. Mikitik, Yu.V. Sharlai, Phys. Rev. B **90**, 155122
15 (2014)
- 16 3. G.P. Mikitik, Yu.V. Sharlai, Fiz. Nizk. Temp. **34**, 1012
17 (2008) [Low Temp. Phys. **34**, 794 (2008)]
- 18 4. Judit Sári, M.O. Goerbig, Csaba Tóke, Phys. Rev. B **92**,
19 035306 (2015)
- 20 5. Takao Morinari, Takami Tohyama, J. Phys. Soc. Jpn **79**,
21 044708 (2010)
- 22 6. Igor Proskurin, Masao Ogata, Yoshikazu Suzumura, Phys.
23 Rev. B **91**, 195413 (2015)
- 24 7. M.O. Goerbig, Rev. Mod. Phys. **83**, 1193 (2011)
- 25 8. Vinu Lukose, R. Shankar, G. Baskaran, Phys. Rev. Lett.
26 **98**, 116802 (2007)
- 27 9. Takao Morinari, Takahiro Himura, Takami Tohyama, J.
28 Phys. Soc. Jpn **78**, 023704 (2009)

10. Naoya Tajima, Takahiro Yamauchi, Tatsuya Yamaguchi, 29
Masayuki Suda, Yoshitaka Kawasaki, Hiroshi M. 30
Yamamoto, Reizo Kato, Yutaka Nishio, Koji Kajita, 31
PRB **88**, 075315 (2013) 32
11. Naoya Tajima, Shigeharu Sugawara, Reizo Kato, Yutaka 33
Nishio, Koji Kajita, Phys. Rev. Lett. **102**, 176403 (2009) 34
12. M. Orlita, P. Neugebauer, C. Faugeras, A.-L. Barra, M. 35
Potemski, F.M.D. Pellegrino, D.M. Basko, Phys. Rev. 36
Lett. **108**, 017602 (2012) 37
13. A.A. Abrikosov, Phys. Rev. B **60**, 4231 (1999) 38
14. I. Lobato, B. Partoens, Phys. Rev. B **83**, 165429 (2011) 39
15. Jae-Kap Lee, Seung-Cheol Lee, Jae-Pyoung Ahn, Soo- 40
Chul Kim, J.I.B. Wilson, P. John, J. Chem. Phys. **129**, 41
234709 (2008) 42
16. I.V. Kozlov, J.C. Medina Pantoja, Fiz. Nizk. Temp. **40**, 43
706 (2014) [Low Temp. Phys. **40**, 547 (2014)] 44
17. M.S. Dresselhaus, G. Dresselhaus, Adv. Phys. **51**, 1 (1980), 45
2002 46
18. A. Grüneis, C. Attacalite, A. Rubio, D.V. Vyalikh, S.L. 47
Molodtsov, J. Fink, R. Follath, W. Eberhardt, B. Büchner, 48
T. Pichler, Phys. Rev. B **80**, 075431 (2009) 49
19. G. Wang, W.R. Datars, P.K. Ummat, Phys. Rev. B **44**, 50
8294 (1991) 51
20. I.M. Lifshitz, M.Ya. Azbel, A.A. Slutskin, Zh. Eksp. Teor. 52
Fiz. **43**, 1464 (1962) [Sov. Phys. J. Exp. Theor. Phys. **16**, 53
1035 (1963)] 54
21. N.M. Temme, J. Appl. Math. Phys. (ZAMP) **41**, 114 55
(1990) 56
22. S. Das Sarma, S. Adam, E.H. Hwang, E. Rossi, Rev. Mod. 57
Phys. **83**, 407 (2011) 58
23. J.W. MacClure, Phys. Rev. **108**, 612 (1957) 59
24. J.C. Slonczewski, P.S. Weiss, Phys. Rev. **109**, 272 (1958) 60
25. N.A. Goncharuk, L. Nádvořník, C. Faugeras, M. Orlita, L. 61
Smrčka, Phys. Rev. B **86**, 155409 (2012) 62
26. S.S. Pershoguba, D.S.L. Abergel, V.M. Yakovenko, A.V. 63
Balatsky, Phys. Rev. B **91**, 085418 (2015) 64
27. Serguei Tchoumakov, M. Civelli, M.O. Goerbig, Phys. 65
Rev. Lett. **117**, 086402 (2016) 66
28. I.V. Kozlov, Juan Sotelo-Campos, J.C. Medina Pantoja, 67
in *Physical phenomena in solids, proceedings of the XII* 68
International Conference, Kharkiv, 2015, edited by V.S. 69
Krilovskiy, V.P. Poyda (V.N. Karasin Kharkiv National 70
University, Kharkiv, Ukraine, 2015), p. 35 71